

Forum Original Research Communication

Application of *In Vivo* ESR/Spin-Probe Technique to Monitor Tumor *In Vivo* in Mouse Footpad

KAZUHIRO ICHIKAWA,¹ EMIKO SAKABE,^{1,4} KEN-ICHIRO KUNINOBU,¹ TAKAO YAMORI,² TAKASHI TSURUO,² TAKASHI YAO,³ MASAZUMI TSUNEYOSHI,³ and HIDEO UTSUMI¹

ABSTRACT

The redox status of tumors inoculated into the footpads of mice was investigated by using an *in vivo* ESR/spin-probe technique. A single-cell suspension of a metastatic subclone of colon carcinoma NL-17 was inoculated into the footpads of Balb/c mice. At 12, 24, 48, and 96 h after the inoculation, a spin probe, either carbamoyl- or carboxy-PROXYL, was intravenously injected, and then the ESR spectra of each footpad were separately obtained under a one-dimensional magnetic-field gradient. The change in the ESR signal intensity of the spin probe was closely related to the tumor volume in the footpads, but no significant difference was observed between carbamoyl- and carboxy-PROXYL. The *in vivo* ESR signal decay of carbamoyl-PROXYL, which is related to the conversion of the nitroxyl radical to hydroxylamine, was enhanced in the inoculated footpads but not in the reference one. The ESR signal decay was not influenced by coadministration of radical scavengers, SOD, catalase, mannitol, or dimethylthiourea, suggesting that the redox status but not reactive oxygen species generation played a role in the enhanced signal decay. *Antioxid. Redox Signal.* 9, 1699–1707.

INTRODUCTION

IT HAS BEEN REPORTED THAT TUMORS have a different redox status than normal tissues, which may result in different responses to radiation therapy (24) or cytotoxic drugs (2). NL-17 is a cell line established from colon cancer in Balb/c mice (37), and is a highly metastatic subclone among a series of subclones. Intravenous or subcutaneous injection of NL-17 caused lung metastatic foci 40 days after injection (37, 47). The redox status in tumor cells could be affected by various factors, including the activities of antioxidative enzymes (1, 4, 9, 17). However, the *in vivo* redox status of the tumor tissue of this subclone had not been investigated.

In vivo electron-spin resonance (*in vivo* ESR)/spin-probe technique is a unique method to investigate *in vivo* free radical reactions (23, 25, 36, 40, 42, 44, 49)/reducing capability non-invasively (7, 13, 20, 45), because the ESR signal-decay rates

of nitroxyl spin probes are susceptible to interaction with *in vivo* redox systems and ROS.

In vivo ESR/spin-probe technique has been used to examine tumor redox status (20, 21, 45). The tests in these reports were carried out at 5–14 days (45) after the inoculation (20, 21), and demonstrated that the tissue became highly reductive within a few weeks after the inoculation of tumor cells. After inoculation into animals, tumor cells experience several stages, including survival, progression, and formation of necrotic areas. The reductive status in the tumor tissue should be different, depending on the period after inoculation, but this remains to be clarified. The *in vivo* ESR/nitroxyl spin-probe technique is quite a powerful tool to monitor redox reactions. To elucidate the sites of the reaction, we used carbamoyl- and carboxy-PROXYL, which are partially membrane-permeable and membrane-impermeable spin probes, respectively (46). The use of multiple spin probes with different permeabilities should have

¹Department of Bio-function Science, Graduate School of Pharmaceutical Sciences, Kyushu University, Kyushu; ²Division of Experimental Chemotherapy, Japanese Foundation for Cancer Research, Tokyo; and ³Department of Anatomic Pathology, Graduate School of Medical Sciences, Kyushu University, Kyushu, Japan.

⁴Present address of M.Sc. Sakabe: Research & Development Division, Mitsubishi Pharma Corporation, Japan.

the capability to monitor site-specific information *in vivo* (38, 40).

We thus designed the current study to investigate changes in the *in vivo* redox status of NL-17 by using spin probes with different permeabilities to examine the sites and changes in redox status a few days after tumor inoculation.

MATERIALS AND METHODS

Chemical compounds

Nitroxyl spin probes, 3-carbamoyl-2,2,5,5-tetramethylpyrrolidine-1-oxyl (carbamoyl-PROXYL) and 3-carboxy-2,2,5,5-tetramethylpyrrolidine-1-oxyl (carboxy-PROXYL) from Aldrich Chemical Co. (St. Louis, MO) were used in the present experiment. The partition coefficients (38) and their chemical structure are shown in Table 1. All other chemicals of highest grade were purchased from Wako Pure Chemicals (Osaka, Japan).

Cell culture

NL-17 was maintained as monolayer culture in RPMI-1640 medium supplemented with 10% fetal bovine serum until injection into mouse footpads.

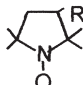
Animal treatment

Female Balb/c mice (5 weeks, 17–19 g) were purchased from Kyudo Co. Ltd. (Fukuoka, Japan) and were kept in 12-h dark/light cycles with *ad libitum* intake of water and chow (MF Oriental Yeast Co., Tokyo, Japan). Animal care was carried out according to our institutional animal research guidelines. Mice were injected subcutaneously in their footpads with a cell suspension of tumor cells (10^6 cells in 0.1 ml phosphate-buffered saline: PBS, unless otherwise noted) while the mice were under very light ether anesthesia. The volume of the footpad was evaluated by sinking the footpad in water and measuring the volume of water excluded (43). The footpad size ratio was calculated by dividing the values of the inoculated footpads with those of reference footpads.

In vivo ESR measurement

At 12, 24, 48, and 96 h after the footpad was inoculated, the spin probe (1 mmol/kg) was injected intravenously. While the mice were under very light halothane anesthesia, the *in vivo* ESR spectra in the footpad region of the hind legs were observed with an L-band ESR spectrometer having a one-dimensional magnetic-

TABLE 1. STRUCTURES AND *n*-OCTANOL/WATER PARTITION COEFFICIENTS OF NITROXYL SPIN PROBES

	Basic structure	R	Po/w (38)
Carbamoyl-PROXYL		–CONH ₂	0.68
Carboxy-PROXYL		–COOH	0.01

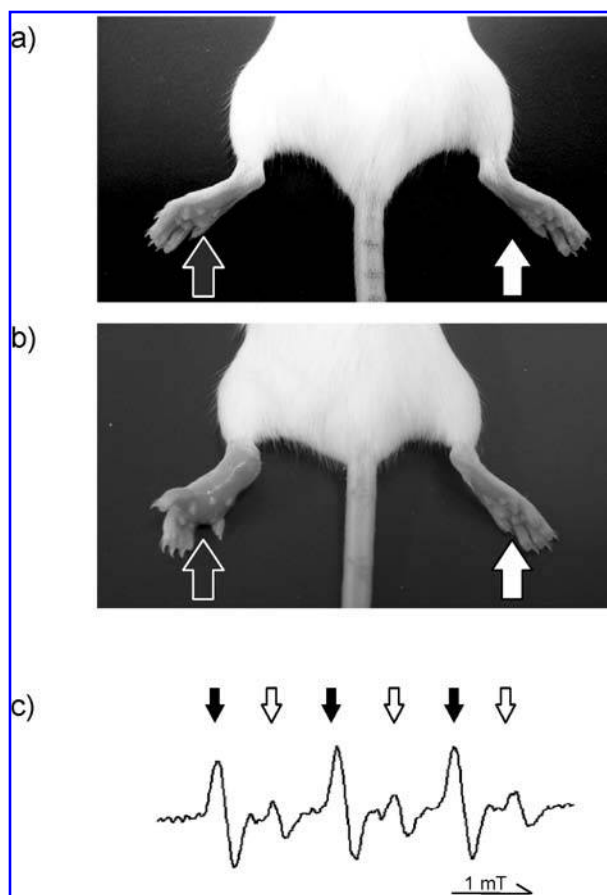


FIG. 1. The change in mouse footpads at (a) day 1, (b) day 6, and (c) *in vivo* ESR spectra of carbamoyl-PROXYL in NL-17-inoculated mice 6 days after the inoculation. NL-17 cells were inoculated into the left footpads of Balb/c mice. The inoculated and reference footpads are indicated with solid and open symbols, respectively. ESR spectra were separately observed under a one-dimensional magnetic field gradient, as described in Materials and Methods.

field gradient (0.5 mT/cm). The typical triplet ESR signals from tumor-inoculated or reference footpads of mice were collected with a PC equipped with an analog digital converter. To avoid the influence of the partial pressure of oxygen (pO_2) on the signal intensity, the ESR spectra were integrated, and the peak areas of the ESR spectra thus calculated were used as the signal intensity. The generation of ROS in the NL-17 inoculated footpads was evaluated by simultaneous injection of radical scavengers and the carbamoyl-PROXYL. Four days after the NL-17 inoculation, mannitol (1.05 mmol/kg BW), dimethylthiourea (DMTU: 1.05 mmol/kg BW), 1,000 U SOD, or 1,000 U catalase was injected intravenously with carbamoyl-PROXYL. The microwave frequency was 1.06 GHz, and the power was 1.0 mW. The amplitude of the 100-kHz field modulations was 0.1 mT. The external magnetic field was swept at a scan rate of 10.0 mT/min.

In vitro ESR measurement

Spin probes (1 mmol/kg) were injected intravenously into each mouse while it was under pentobarbital anesthesia. Five

minutes after the injection, the mouse was killed by transcardiac perfusion of 50 ml of 0.9% saline, and both footpads were removed, homogenized in a cryostat (Microtec Niton Ltd., Chiba, Japan), and then suspended in a deoxygenated saline solution. The ESR signal of the nitroxyl probe in the suspension was then measured both before and after reoxidation with potassium ferricyanide by using an X-band ESR spectrometer with DPPH as an intensity standard. The magnetic field was 336.0 ± 5.0 mT. The microwave frequency was ~ 9.44 GHz, and the power was 5.0 mW. The amplitude of the 100-kHz field modulation was 0.1 mT. The external magnetic field was swept at a scan rate of 10.0 mT/min.

Tissue permeability

The tissue permeability was evaluated by using Evans blue dye as the marker (33). The Evans blue solution (4% Evans blue, 50 μ l) was intravenously administered to the mouse while it was under pentobarbital anesthesia. Ten minutes after the injection, the mouse was killed by transcardiac perfusion of 0.9% saline, both footpads were incubated in formamide solution for 72 h at 37°C, and then the Evans blue dye was extracted. The absorbance of the extract was measured at 620 nm by using a spectrophotometer.

Statistical analysis

Data were analyzed by Student's *t* test or one-way ANOVA (StatView, SAS). The results were expressed as a mean \pm SD, and the significance level was defined as $p < 0.05$.

RESULTS

Time course of tumor growth

Figure 1a shows the typical change in the footpad after the inoculation. As shown in Fig. 1b, the thickness of the footpad inoculated with NL-17 increased gradually, but not in

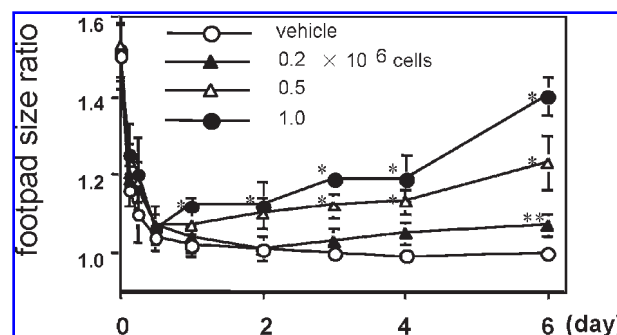


FIG. 2. Time course of footpad-size ratio after NL-17 inoculation. Footpad size was measured 3, 6, and 12 h and 1, 2, 3, 4, and 6 days after inoculation with 0, 0.2, 0.5, and 1.0×10^6 cells, as described in the Materials and Methods. Values in the vertical axis were the ratios calculated by dividing the values of the inoculated footpads with that of reference footpads. All values represent means of four mice \pm SD. ** $p < 0.05$; * $p < 0.01$.

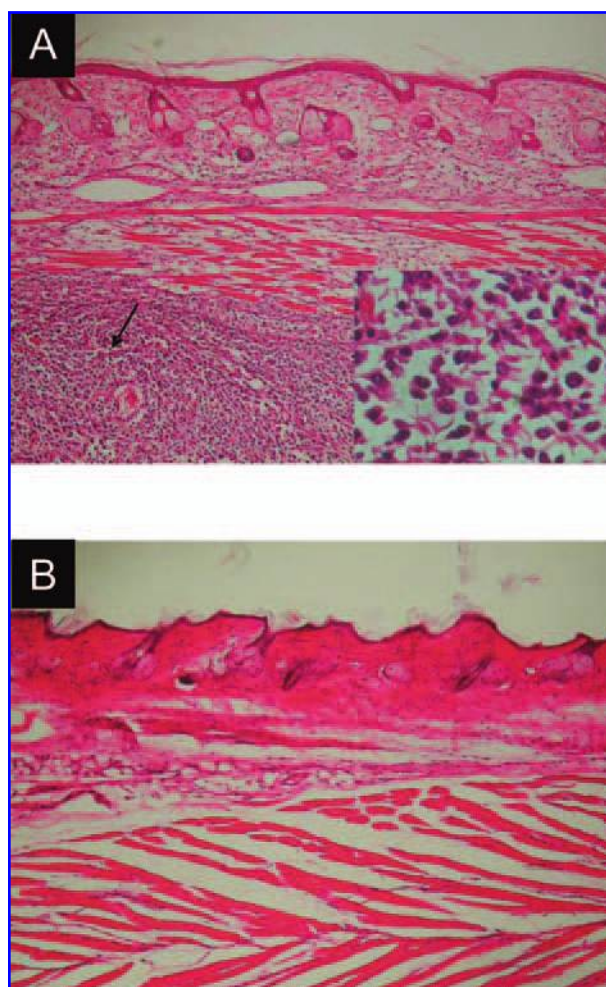


FIG. 3. Hematoxylin-eosin staining of (a) NL-17-inoculated or (b) reference footpad. Four days after NL-17 inoculation, mice were killed, and their footpads were removed. The histologic changes were evaluated by using standard hematoxylin-eosin stain. Arrows, Tumor area. (Magnification: $\times 200$; $\times 1,000$ for inset.)

those treated with vehicle solution. The tumor growth after inoculation was evaluated by using its footpad volume. The footpad volume increased transiently after the injection in both the tumor-inoculated and vehicle-injected groups (Fig. 2), presumably because of the volume of the injection. The footpad volume of the vehicle-injected footpad returned to the reference level within 12 h. The volume of untreated footpads (reference) was between 0.13 and 0.17 ml for footpads without tumor injection. Afterward, the changes in footpad volume were represented as the footpad-size ratio between the reference and tumor footpads in each animal. In the NL-17-inoculated group, the footpad-size ratio gradually increased in a cell number-dependent manner (see Fig. 2). Figure 3 shows a light microscopic photograph of typical hematoxylin/eosin-stained reference and tumor tissue in a mouse footpad 4 days after inoculation of 1.0×10^6 NL-17 cells. The photograph shows that NL-17 cells formed a large tumor area in the footpad, even though inflammatory cells were not evident at this point.

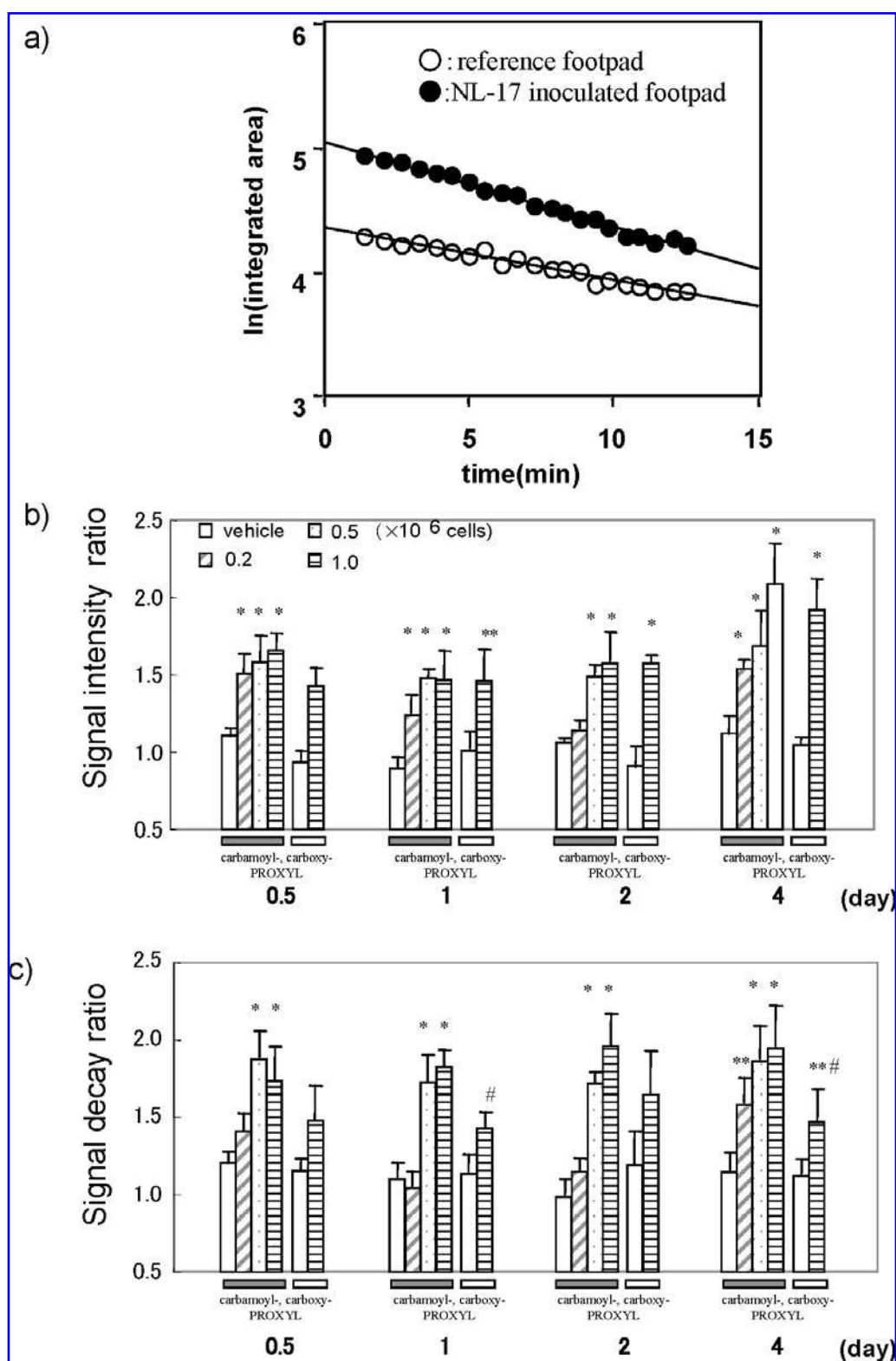


FIG. 4. The changes in the ESR signal intensity and decay rate in NL-17-inoculated mouse footpads. (a) Semilogarithmic plot of the typical signal intensity after intravenous injection of spin probe; (b) time course of signal-intensity ratio; and (c) signal-decay ratio after NL-17 inoculation. The cells ($0, 0.2, 0.5$, and 1.0×10^6 cells) were inoculated into Balb/c mice; and $0.5, 1, 2$, and 4 days after the inoculation, carbamoyl- or carboxy-PROXYL was injected as the spin probe. The ratios of the signal intensity and the decay rates were calculated as described in Materials and Methods. All values represent means of four mice \pm SD. ** $p < 0.05$; * $p < 0.01$ between vehicle and tumor group. # $p < 0.05$ between groups injected with carbamoyl- and carboxy-PROXYL.

TABLE 2. TIME COURSE OF TUMOR SIZE AND SPIN PROBE REDUCTION IN FOOTPAD AFTER NL-17 INOCULATION

	Day 4	Day 7	Day 14	Day 21
Tumor size ratio	1.2 ± 0.1	1.5 ± 0.1	4.1 ± 0.2	7.8 ± 0.3
Signal decay ratio	1.89 ± 0.15	1.81 ± 0.21	1.43 ± 0.14	0.83 ± 0.11

Tumor size and reduction rates of carbamoyl-PROXYL was observed in reference and tumor footpads with 1.0×10^6 cells at Day 4, 7, 14 and 21. The data represented the ratio of either tumor size or signal decay rates between reference and tumor footpads. Number of animal at each data points was three.

ESR signal intensities in footpad and their decay

Typical ESR spectra under 1-D field gradient are shown in Fig. 1c. It was reported that tumor oxygen concentration is heterogeneous with BOLD MRI or ESR oxymetry (3, 5, 20). It is well known that the paramagnetic oxygen molecule broadens the ESR linewidth of the spin probe (6) and that the line-broadening due to oxygen is used to measure tissue pO_2 (16).

A semilogarithmic plot of ESR signal intensity from the ESR spectrum area versus time (after injection of the spin probe) obeyed quasi-first-order decay for carbamoyl-PROXYL (28) (Fig. 4a). The amount of spin probe in the region was evaluated from a vertical intercept of the decay curve. The ratios between the inoculated and reference footpad of an individual mouse were calculated to reduce the experimental variance among mice. The ratio in the NL-17-inoculated group decreased within 24 h after the injection and gradually increased again for both PROXYLs, depending on the number of cells inoculated and time after inoculation (see Fig. 4b).

The ESR signal decay of carbamoyl-PROXYL was significantly enhanced in the NL-17 group (see Fig. 4c). The signal decay in the footpad of the group injected with 0.2×10^6 cells initially returned to the vehicle level 24 h after the inoculation, but then gradually increased again. The group inoculated with 0.5 and 1.0×10^6 cells demonstrated significant enhancement of the signal decay 12 h after the inoculation and kept the high decay level until at least 96 h. The tumor-size ratio increased after the inoculation in a time-dependent manner, but the signal-decay ratio decreased from 1.89 at day 4 to 1.43 at day 14 and 0.83 at day 21. The signal-decay rate in the tumor on day 21 was smaller than that in the reference footpad. Yamada *et al.* (20) observed the spatial distribution and the reduction of carbamoyl-PROXYL in footpads with 1.0×10^6 RIF-1 tumor cells at 5, 7, 12, and 14 days, and reported that the reduction

rate was enhanced in the tumor footpad at day 7 and then decreased at day 14. Our observations, shown in Table 2, agreed with previous report (20).

We focused our study on the redox state of footpads with NL-17 up to day 4, where the signal-decay ratio of carbamoyl-PROXYL was dependent on the number of cells inoculated (see Fig. 4c). The signal-decay ratio of carboxy-PROXYL was less enhanced than that obtained with carbamoyl-PROXYL (see Fig. 4c). The decay rates in both footpads were not significantly different in vehicle-injected mice. It is noteworthy that the enhanced signal decay was observed only when viable NL-17 cells were injected into the footpad. No enhancement of signal decay was observed when cell fragments of NL-17, prepared by mild sonication of the cell suspension, were injected (Table 3).

To examine the involvement of ROS generation in the signal-decay enhancement from the NL-17-inoculated footpad, ESR experiments were carried out by injecting various antioxidants along with the spin probes. This can reportedly suppress the signal decay competitively. Neither dimethylthiourea, which is a membrane-permeable hydroxyl radical scavenger, nor mannitol, which is membrane-impermeable, suppressed the enhanced decay (Fig. 5). Catalase and Cu,Zn-SOD also did not affect the signal-decay ratio. The data indicated that the enhancement of the signal decay observed in NL-17-inoculated footpads for 4 days was probably not related to ROS generation but might have been due to a change in redox status.

Tissue permeability and decay of the spin probe

Changes in the tissue permeability in NL-17-inoculated footpads may be another cause for the enhanced signal decay. The spin probe may encounter highly active reducing enzymes (32, 34) or a high concentration of ascorbate (27, 30), which would

TABLE 3. EFFECT OF SONICATION OF NL17 CELLS ON THE SPIN PROBE REDUCTION

	Vehicle	NL-17	Sonication	Sonication autoclave
Signal decay ratio	0.95 ± 0.15	1.38 ± 0.13	0.89 ± 0.09	0.83 ± 0.12

Signal reduction rates of carbamoyl-PROXYL were observed in reference and tumor footpads at Day 4. NL-17 (1×10^6 cells) were sonicated for 30 sec, twice, on ice. For the autoclave group, the cell suspension was autoclaved at 121°C for 3 min after the sonication. The data represented the ratio of signal decay rates between reference and treated footpads. Number of animals at each data point was three.

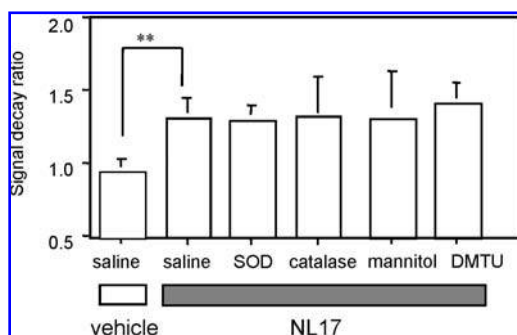


FIG. 5. The effect of simultaneous injection of antioxidants on the enhanced signal decay in NL-17-inoculated footpads. Four days after the inoculation, mannitol, DMTU, SOD, or catalase was intravenously injected with carbamoyl-PROXYL, as described in the Materials and Methods. All values represent means of four to five mice \pm SD. $**p < 0.05$.

reduce the spin probe to its hydroxylamine form, which makes the spin probe more permeable to the tissue. Therefore, tissue permeability in the NL-17-inoculated footpads was examined by using Evans blue dye extravasations. Tissue permeability increased in both the vehicle and the NL-17-inoculated footpads within a day after the inoculations, presumably because of the effects of needle insertion during the injection process (Fig. 6). At 96 h after inoculation, only the NL-17-inoculated footpads showed a significant increase in permeability, but this was not true in the vehicle-injected ones.

The conversion of carbamoyl-PROXYL to the hydroxylamine form

Reduction of the nitroxyl form of carbamoyl-PROXYL to its hydroxylamine form was quantified from the tissue region of the footpad by using X-band ESR spectroscopy. The ESR signal intensities of the tissue homogenates before potassium ferricyanide treatment were almost the same between the vehicle-inoculated and NL-17 cell-inoculated group, but a significant increment was observed in the signal intensity of the NL-17 cell-inoculated group after treatment with potassium ferricyanide. The total amount of carbamoyl-PROXYL, intact and hydroxylamine forms, was larger in the NL-17 footpads than in the reference footpads of the same mice (Fig. 7). It should be mentioned that signal intensities were 1.82 times larger after reoxidation with potassium ferricyanide in tumor footpads than in reference footpads, which was close to the signal-intensity ratio in Fig. 4b. The percentage of hydroxylamine was significantly larger in the inoculated footpads than the reference footpads (*i.e.*, $86.3 \pm 1.8\%$ and $67.6 \pm 5.5\%$ for the NL-17-inoculated and reference footpads, respectively).

DISCUSSION

Free radical generation and tissue redox status reportedly have important roles in tumor cells (22, 29) or tissues (26). *In*

vivo ESR measurement of tumors in animals is therefore regarded as an important tool, especially for tumor oximetry (3, 5, 11, 15, 19, 41) and monitoring tumor redox status (14, 20, 21). A combination of nitroxyl spin probes with different functional groups becomes a powerful tool with which to examine site-specific ROS generation or redox changes (40, 46). We recently demonstrated that the combination of two spin probes, labeled with ^{14}N or ^{15}N , with different functional groups, enabled us to investigate redox reactions in the domains separated by membranes at a nanometer scale by using Overhauser-enhanced MRI (39). Changes in the tumor redox status have been reported in the literature by using an *in vivo* ESR/spin probe (14, 20, 21), but this was not examined by using multiple spin probes. We therefore used two spin probes, carbamoyl- and carboxy-PROXYL, in this study to evaluate the site-specific redox changes *in vivo* in NL-17 tumor cells inoculated into mouse footpads.

NL-17 cells were grown in Balb/c mouse footpads (Figs. 2 and 3), as reported previously (47). The amount of both carbamoyl- and carboxy-PROXYL in the footpad regions of NL-17-inoculated mice significantly increased despite the difference in their membrane permeability. The amount of the spin probes in the footpads was in good correlation with the footpad volumes, and their correlation coefficients were 0.831 and 0.792 for carbamoyl- and carboxy-PROXYL, respectively. The

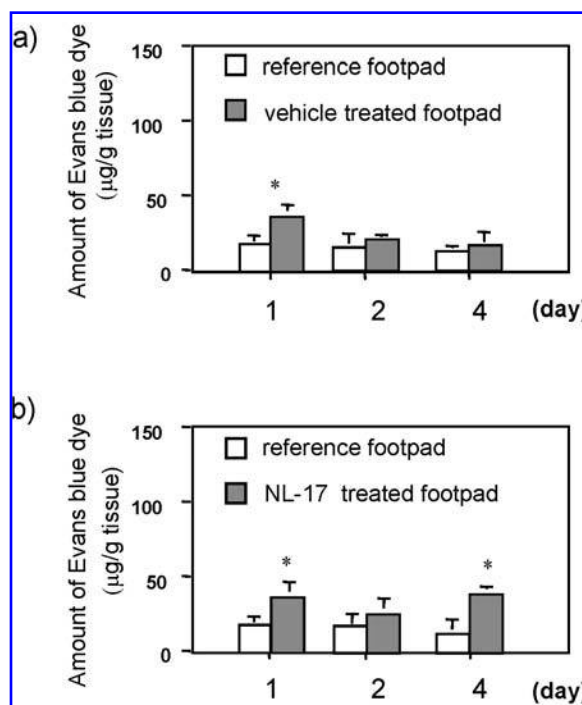
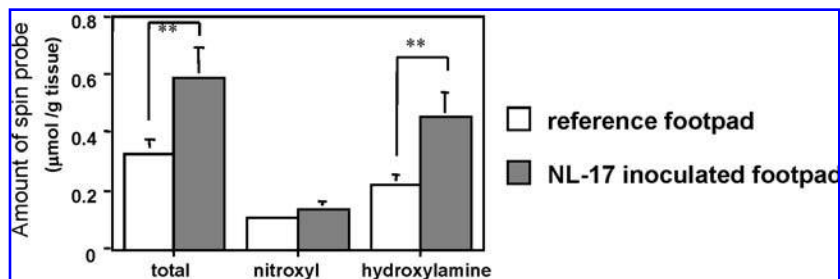


FIG. 6. The vessel permeability evaluated by Evans blue dye extravasation. Either the vehicle or 1.0×10^6 NL-17 cells were injected. Evans blue dye was intravenously injected into mice, and the dye was extracted from mouse footpads injected with (a) vehicle or (b) NL-17 cells, as described in the Materials and Methods. All values represent means of three to four mice \pm SD. $*p < 0.01$

FIG. 7. The amount of nitroxyl and hydroxylamine forms of carbamoyl-PROXYL in NL-17-inoculated and reference footpads. The probe was administered intravenously 4 days after the inoculation. Five minutes after spin-probe administration, mice were perfused with PBS, and both footpads were rapidly frozen with liquid nitrogen. The amount of nitroxyl radicals was quantified by using X-band ESR, as described in the Material and Methods. After re-oxidation with potassium ferricyanide, the total amount of spin probe was obtained. All values represent means of five to seven mice \pm SD. $**p < 0.05$.



amount of the spin probes was also in good correlation with the amount of Evans blue dye in the tumor, and the correlation coefficients were 0.903 and 0.883 for carbamoyl- and carboxy-PROXYL, respectively (Figs. 2 and 6). These results might be due to tumor growth, which results in increased vessel and distribution volumes, because angiogenesis proceeds along with tumor growth.

In contrast, the decay rates of the spin probe in tumor footpads showed different profiles between the probes. The decay rates of carbamoyl-PROXYL were enhanced in the footpad inoculated with NL-17 cells in a dose- and time-dependent manner and correlated with footpad volumes (Figs. 2 and 4c), whereas that of carboxy-PROXYL in tumor footpads was not significant, indicating that the inoculation of NL-17 cells produced a reductive state in the tissue.

We previously reported, by using an animal model for gastric ulcers, that membrane-permeable and impermeable spin probes had differential effects in both spin-probe reduction and ulcer suppression (40). When spin probes are permeable to tissue, which is rich in reducing enzymes (32, 34), it would result in a higher likelihood that nitroxyl spin probes would encounter a reducing environment *in vivo*. Carbamoyl-PROXYL can partially penetrate into the surface of the tissue and can be reduced to its hydroxylamine form (12), whereas carboxyl-PROXYL is membrane impermeable. Evans blue dye is permeable to the extracellular domain of the tissue for a short time (8, 18), although the region is poor in reducing species. In the current study, tissue permeability, which was evaluated by the Evans blue method, increased on day 4 after inoculation (see Fig. 6). However, the signal decay of carboxy-PROXYL was not affected by the increased tissue permeability, presumably because carboxy-PROXYL could not penetrate into the parenchymal domain.

The total amount of carbamoyl-PROXYL in the tumor footpads increased in accordance with signal-intensity ratios (Figs. 4 and 7), supporting the fact that carbamoyl-PROXYL was permeable to the tumor domain. The amount of the hydroxylamine form of the probe was larger in the tumor group than in the vehicle group, indicating that the reduction of carbamoyl-PROXYL was elevated in the tumor tissue (see Fig. 4). These results of enhanced signal intensity and diverse signal decays between carbamoyl- and carboxy-PROXYL supported the hypothesis that the enhanced signal decay of carbamoyl-PROXYL

observed in this study occurred in the tumor domain of NL-17-injected footpads.

The enhanced signal decay of spin probes could also have been influenced by several processes, including elevated ROS formation (10, 25, 31), reduction with redox enzymes, formation of a hypoxic tumor region (20), and the suppression of the reoxidation from the hydroxylamine to the nitroxyl form. In various oxidative diseases, elevation of reactive oxygen species generation was monitored by the *in vivo* ESR/spin-probe technique where the administration of radical scavengers or antioxidants suppressed the enhanced signal decay competitively (35, 40, 46, 48). In the current study, we examined the effects of radical scavengers on the enhanced signal decay caused by the NL-17 inoculation. These scavengers, surprisingly, did not affect the ESR signal decay (see Fig. 5), indicating that the ROS-generation level in the tumor domain was negligible, if any. This result was further supported by the absence of inflammatory cells, which are known to generate ROS, in the tumor domain (see Fig. 3).

In summary, we used spin probes with different tissue permeabilities and showed that *in vivo* tumor growth was well correlated with the ESR signal intensity of both the membrane-permeable and impermeable spin probes, but *in vivo* tumor redox was detectable only with carbamoyl-PROXYL, which is partially membrane permeable. A higher reductive state was observed in the tissue domain of viable NL-17-inoculated footpads, with carbamoyl-PROXYL but not with carboxy-PROXYL, which was most likely due to the changes in redox status. The *in vivo* redox-status monitoring of tumor tissue with a combination of spin probes would be useful for obtaining information from tumor biology.

ACKNOWLEDGMENTS

This work was supported by the Grant-in-Aid for Scientific Research (A) from JSPS (Japan Society for the Promotion of Science), and for Scientific Research on Priority Areas "Application of Molecular Spins" from the Ministry of Education, Culture, Sports, Science and Technology of Japan, and by 21st Century Centers of Excellence (COE) program of Kyushu University from the Ministry of Education, Culture, Sports, Science and Technology of Japan.

ABBREVIATIONS

carbamoyl-PROXYL, 3-carbamoyl-2,2,5,5-tetramethylpyrrolidine-1-oxyl; carboxy-PROXYL, 3-carboxy-2,2,5,5-tetramethylpyrrolidine-1-oxyl; ESR, electron spin resonance; ROS, reactive oxygen species; SOD, superoxide dismutase.

REFERENCES

- Bostwick DG, Alexander EE, Singh R, Shan A, Qian J, Santella RM, Oberley LW, Yan T, Zhong W, Jiang X, and Oberley TD. Antioxidant enzyme expression and reactive oxygen species damage in prostatic intraepithelial neoplasia and cancer. *Cancer* 89: 123–134, 2000.
- Davis W Jr, Ronai Z, and Tew KD. Cellular thiols and reactive oxygen species in drug-induced apoptosis. *J Pharmacol Exp Ther* 296: 1–6, 2001.
- Dunn JF, O'Hara JA, Zaim-Wadghiri Y, Lei H, Meyerand ME, Grinberg OY, Hou H, Hoopes PJ, Demidenko E, and Swartz HM. Changes in oxygenation of intracranial tumors with carbogen: a BOLD MRI and EPR oximetry study. *J Magn Reson Imaging* 16: 511–521, 2002.
- Durak I, Perk H, Kavutcu M, Canbolat O, Akyol O, and Beduk Y. Adenosine deaminase, 5'-nucleotidase, xanthine oxidase, superoxide dismutase, and catalase activities in cancerous and noncancerous human bladder tissues. *Free Radic Biol Med* 16: 825–831, 1994.
- Elas M, Williams BB, Parasca A, Mailer C, Pelizzari CA, Lewis MA, River JN, Karczmar GS, Barth ED, and Halpern HJ. Quantitative tumor oxymetric images from 4D electron paramagnetic resonance imaging (EPRI): methodology and comparison with blood oxygen level-dependent (BOLD) MRI. *Magn Reson Med* 49: 682–691, 2003.
- Gallez B, Bacic G, Goda F, Jiang J, O'Hara JA, Dunn JF, and Swartz HM. Use of nitroxides for assessing perfusion, oxygenation, and viability of tissues: in vivo EPR and MRI studies. *Magn Reson Med* 35: 97–106, 1996.
- Gomi F, Utsumi H, Hamada A, and Matsuo M. Aging retards spin clearance from mouse brain and food restriction prevents its age-dependent retardation. *Life Sci* 52: 2027–2033, 1993.
- Green TP, Johnson DE, Marchessault RP, and Gatto CW. Transvascular flux and tissue accrual of Evans blue: effects of endotoxin and histamine. *J Lab Clin Med* 111: 173–183, 1988.
- Guner G, Islekel H, Oto O, Hazan E, and Acikel U. Evaluation of some antioxidant enzymes in lung carcinoma tissue. *Cancer Lett* 103: 233–239, 1996.
- Han JY, Takeshita K, and Utsumi H. Noninvasive detection of hydroxyl radical generation in lung by diesel exhaust particles. *Free Radic Biol Med* 30: 516–525, 2001.
- He J, Beghein N, Ceroke P, Clarkson RB, Swartz HM, and Gallez B. Development of biocompatible oxygen-permeable films holding paramagnetic carbon particles: evaluation of their performance and stability in EPR oximetry. *Magn Reson Med* 46: 610–614, 2001.
- Ichikawa K, Sato Y, Kondo H, and Utsumi H. An ESR contrast agent is transported to rat liver through organic anion transporter. *Free Radic Res* 40: 403–408, 2006.
- Ilangovan G, Li H, Zweier JL, Krishna MC, Mitchell JB, and Kuppusamy P. *in vivo* measurement of regional oxygenation and imaging of redox status in RIF-1 murine tumor: effect of carbogen-breathing. *Magn Reson Med* 48:723–730, 2002.
- Ilangovan G, Li H, Zweier JL, and Kuppusamy P. *In vivo* measurement of tumor redox environment using EPR spectroscopy. *Mol Cell Biochem* 234–235: 393–398, 2002.
- Ilangovan G, Manivannan A, Li H, Yanagi H, Zweier JL, and Kuppusamy P. A naphthalocyanine-based EPR probe for localized measurements of tissue oxygenation. *Free Radic Biol Med* 32: 139–147, 2002.
- Inoue M, Utsumi H, and Kirino Y. A comparative ESR study of some paramagnetic materials as probes for the noninvasive measurement of dissolved oxygen in biological systems. *Chem Pharm Bull (Tokyo)* 42: 2346–2348, 1994.
- Kahlos K, Pitkanen S, Hassinen I, Linnainmaa K, and Kinnula VL. Generation of reactive oxygen species by human mesothelioma cells. *Br J Cancer* 80: 25–31, 1999.
- Kawada T, Masui F, Tezuka A, Ebisawa T, Kumagai H, Nakazawa M, and Toyo-Oka T. A novel scheme of dystrophin disruption for the progression of advanced heart failure. *Biochim Biophys Acta* 1751: 73–81, 2005.
- Krishna MC, English S, Yamada K, Yoo J, Murugesan R, Devasahayam N, Cook JA, Golman K, Ardenkjaer-Larsen JH, Subramanian S, and Mitchell JB. Overhauser enhanced magnetic resonance imaging for tumor oximetry: coregistration of tumor anatomy and tissue oxygen concentration. *Proc Natl Acad Sci U S A* 99: 2216–2221, 2002.
- Kuppusamy P, Afeworki M, Shankar RA, Coffin D, Krishna MC, Hahn SM, Mitchell JB, and Zweier JL. *in vivo* electron paramagnetic resonance imaging of tumor heterogeneity and oxygenation in a murine model. *Cancer Res* 58: 1562–1568, 1998.
- Kuppusamy P, Li H, Ilangovan G, Cardounel AJ, Zweier JL, Yamada K, Krishna MC, and Mitchell JB. Noninvasive imaging of tumor redox status and its modification by tissue glutathione levels. *Cancer Res* 62: 307–312, 2002.
- Lam EW, Zwacka R, Seftor EA, Nieva DR, Davidson BL, Engelhardt JF, Hendrix MJ, and Oberley LW. Effects of antioxidant enzyme overexpression on the invasive phenotype of hamster cheek pouch carcinoma cells. *Free Radic Biol Med* 27: 572–579, 1999.
- Lee MC, Shoji H, Miyazaki H, Yoshino F, Hori N, Toyoda M, Ikeda Y, Anzai K, Ikota N, and Ozawa T. Assessment of oxidative stress in the spontaneously hypertensive rat brain using electron spin resonance (ESR) imaging and *in vivo* L-Band ESR. *Hypertens Res* 27: 485–92, 2004.
- Mitchell JB and Russo A. The role of glutathione in radiation and drug induced cytotoxicity. *Br J Cancer Suppl* 8: 96–104, 1987.
- Miyazaki H, Shoji H, and Lee MC. Measurement of oxidative stress in stroke-prone spontaneously hypertensive rat brain using *in vivo* electron spin resonance spectroscopy. *Redox Rep* 7: 260–265, 2002.
- Monte M, Davel LE, and de Lustig ES. Inhibition of lymphocyte-induced angiogenesis by free radical scavengers. *Free Radic Biol Med* 17: 259–266, 1994.
- Morris S, Sosnovsky G, Hui B, Huber CO, Rao NU, and Swartz HM. Chemical and electrochemical reduction rates of cyclic nitroxides (nitroxyls). *J Pharm Sci* 80: 149–152, 1991.
- Nishino N, Yasui H, and Sakurai H. *In vivo* L-band ESR and quantitative pharmacokinetic analysis of stable spin probes in rats and mice. *Free Radic Res* 31: 35–51, 1999.
- Nonaka Y, Iwagaki H, Kimura T, Fuchimoto S, and Orita K. Effect of reactive oxygen intermediates on the *in vitro* invasive capacity of tumor cells and liver metastasis in mice. *Int J Cancer* 54: 983–986, 1993.
- Okazaki M and Kuwata K. A stopped-flow ESR study on the reactivity of some nitroxide radicals with ascorbic acid in the presence of beta-cyclodextrin. *J Phys Chem* 89: 4437–4440, 1985.
- Phumala N, Ide T, and Utsumi H. Noninvasive evaluation of *in vivo* free radical reactions catalyzed by iron using *in vivo* ESR spectroscopy. *Free Radic Biol Med* 26: 1209–1217, 1999.
- Quintanilha AT and Packer L. Surface localization of sites of reduction of nitroxide spin-labeled molecules in mitochondria. *Proc Natl Acad Sci U S A* 74: 570–574, 1977.
- Reichman HR, Farrell CL, and Del Maestro RF. Effects of steroids and nonsteroid anti-inflammatory agents on vascular permeability in a rat glioma model. *J Neurosurg* 65: 233–237, 1986.
- Rosen GM and Rauckman EJ. Formation and reduction of a nitroxide radical by liver microsomes. *Biochem Pharmacol* 26: 675–679, 1977.
- Sonta T, Inoguchi T, Matsumoto S, Yasukawa K, Inuo M, Tsubouchi H, Sonoda N, Kobayashi K, Utsumi H, and Nawata H. *in vivo* imaging of oxidative stress in the kidney of diabetic mice and its normalization by angiotensin II type 1 receptor blocker. *Biochem Biophys Res Commun* 330: 415–422, 2005.

36. Takeshita K, Takajo T, Hirata H, Ono M, and Utsumi H. *in vivo* oxygen radical generation in the skin of the protoporphyria model mouse with visible light exposure: an L-band ESR study. *J Invest Dermatol* 122: 1463–470, 2004.
37. Tsuruo T, Kawabata H, Iida H, and Yamori T. Tumor-induced platelet aggregation and growth promoting factors as determinants for successful tumor metastasis. *Clin Exp Metastasis* 4: 25–33, 1986.
38. Utsumi H, Sano H, Naruse M, Matsumoto K, Ichikawa K, and Oi T. Nitroxyl probes for brain research and their application to brain imaging. *Methods Enzymol* 352: 494–506, 2002.
39. Utsumi H, Yamada K, Ichikawa K, Sakai K, Kinoshita Y, Matsumoto S, and Nagai M. Simultaneous molecular imaging of redox reactions monitored by Overhauser-enhanced MRI with ¹⁴N- and ¹⁵N-labeled nitroxyl radicals. *Proc Natl Acad Sci U S A* 103: 1463–1468, 2006.
40. Utsumi H, Yasukawa K, Soeda T, Yamada K, Shigemi R, Yao T, and Tsuneyoshi M. Non-invasive mapping of reactive oxygen species by *in vivo* electron spin resonance spectroscopy in indomethacin-induced gastric ulcers in rats. *J Pharmacol Exp Ther* 317: 228–235, 2006.
41. Velan SS, Spencer RG, Zweier JL, and Kuppusamy P. Electron paramagnetic resonance oxygen mapping (EPROM): direct visualization of oxygen concentration in tissue. *Magn Reson Med* 43: 804–849, 2000.
42. Yamada K, Inoue D, Matsumoto S, and Utsumi H. *in vivo* measurement of redox status in streptozotocin-induced diabetic rat using targeted nitroxyl probes. *Antioxid Redox Signal* 6: 605–611, 2004.
43. Yamada K, Nakamura T, and Utsumi H. Enhanced intraarticular free radical reactions in adjuvant arthritis rats. *Free Radic Res* 40: 455–460, 2006.
44. Yamada K, Yamamiya I, and Utsumi H. In vivo detection of free radicals induced by diethylnitrosamine in rat liver tissue. *Free Radic Biol Med* 40: 2040–2046, 2006.
45. Yamada KI, Kuppusamy P, English S, Yoo J, Irie A, Subramanian S, Mitchell JB, and Krishna MC. Feasibility and assessment of non-invasive *in vivo* redox status using electron paramagnetic resonance imaging. *Acta Radiol* 43: 433–440, 2002.
46. Yamato M, Egashira T, and Utsumi H. Application of *in vivo* ESR spectroscopy to measurement of cerebrovascular ROS generation in stroke. *Free Radic Biol Med* 35: 1619–1631, 2003.
47. Yamori T, Iida H, Tsukagoshi S, and Tsuruo T. Growth stimulating activity of lung extract on lung-colonizing colon 26 clones and its partial characterization. *Clin Exp Metastasis* 6: 131–139, 1988.
48. Yasukawa K, Kasazaki K, Hyodo F, and Utsumi H. Non-invasive analysis of reactive oxygen species generated in rats with water immersion restraint-induced gastric lesions using *in vivo* electron spin resonance spectroscopy. *Free Radic Res* 38: 147–155, 2004.
49. Yoshida M, Saegusa Y, Fukuda A, Akama Y, and Owada S. Measurement of radical-scavenging ability in hepatic metallothionein of rat using *in vivo* electron spin resonance spectroscopy. *Toxicology* 213: 74–80, 2005.

Address reprint requests to:

Hideo Utsumi

Graduate School of Pharmaceutical Sciences

Kyushu University

3-1-1 Maidashi

Fukuoka 812-8582, Japan

E-mail: utsumi@pch.phar.kyushu-u.ac.jp

Date of first submission to ARS Central, April 22, 2007; date of final revised submission, May 16, 2007; date of acceptance, May 21, 2007.

This article has been cited by:

1. Kazuhiro Ichikawa, Keiji Yasukawa. 2012. Imaging in vivo redox status in high spatial resolution with OMRI. *Free Radical Research* **46**:8, 1004-1010. [[CrossRef](#)]
2. David Bardelang, Micaël Hardy, Olivier Ouari, Paul Tordo Spin Labels and Spin Probes . [[CrossRef](#)]
3. Keiji Yasukawa , Kenichi Yamada , Kazuhiro Ichikawa , Hideo Utsumi In Vivo ESR/Spin Probe Technique 90-99. [[Abstract](#)] [[Summary](#)] [[Full Text PDF](#)] [[Full Text PDF with Links](#)]
4. Kazuhiro ICHIKAWA, Ken-ichi YAMADA, Keiji YASUKAWA, Hideo UTSUMI. 2009. Analysis of In vivo Redox Status with Magnetic Resonance Technique. *YAKUGAKU ZASSHI* **129**:3, 273-278. [[CrossRef](#)]
5. Dipak K. Das Methods in Redox Signaling . [[Citation](#)] [[Full Text HTML](#)] [[Full Text PDF](#)] [[Full Text PDF with Links](#)]